Cell Proliferation

*Cell Prolif.* 2008, **41**, 625–644 doi: 10.1111/j.1365-2184.2008.00543.x

# Proteomic analysis of human bone marrow mesenchymal stem cells transduced with human telomerase reverse transcriptase gene during proliferation

G. P. Huang*,**, Z. J. Pan*,†,**, J. P. Huang‡, J. F. Yang*, C. J. Guo*, Y. G. Wang§, Q. Zheng†, R. Chen*, Y. L. Xu*, G. Z. Wang*, Y. M. Xi*, D. Shen¶, J. Jin¶ and J. F. Wang*

**College of Life Sciences, Zhejiang University, Hangzhou, China, †The Second Affiliated Hospital, Zhejiang University, Hangzhou, China, ‡Department of Chemistry, Fudan University, Shanghai, China, §College of Life Sciences, Zhejiang Sci-Tech University, Hangzhou, China, and ¶The First Affiliated Hospital, Zhejiang University, Hangzhou, China*

*Received* 4 *September* 2007*; revision accepted* 19 *November* 2007

**Abstract.** *Objectives*: Previous studies have reported immortalization and tumorigenicity of human mesenchymal stem cells (hMSCs) transduced with exogenous human telomerase reverse transcriptase (hTERT). We also have established a line of hMSCs transduced with hTERT (hTERT–hMSCs) and we have cultured these cells for 290 population doublings (PDs) during which they demonstrated a large proliferation potential but with no tumorigenicity. The aim of this study was to investigate the protein expression profile of hTERT–hMSCs with two-dimensional gel electrophoresis and peptide mass fingerprinting by matrix-assisted laser desorption/ionization time-of-flight mass spectrometry, to be able to analyse the effects of exogenous hTERT on protein expression in hMSCs. *Materials and methods*: We generated proteome maps of primary hMSCs and hTERT–hMSCs at PD 95 and PD 275. *Results*: A total of 1543 ± 145 protein spots in gels of primary MSCs at PD 12, 1611 ± 186 protein spots in gels of hTERT–hMSCs at PD 95 and 1451 ± 126 protein spots in gels of hTERT–hMSCs at 275 PD were detected. One hundred of these were successfully identified, including 20 which were differentially expressed. *Conclusions*: The results suggest that sustaining levels of prohibitin and p53 expression along with differential expression of proteins in hTERT–hMSCs provide an insight into lack of transforming activity of hTERT–hMSCs during cell proliferation.

## INTRODUCTION

Human mesenchymal stem cells (hMSCs) have self-renewal capability and multiple potential for differentiation into a variety of mesenchymal cell lineages such as to osteoblasts, chondrocytes

Correspondence: Jin Fu Wang, Institute of Cell Biology, College of Life Sciences, Zi Jin Gang Campus, Zhejiang University, Hangzhou, Zhejiang 310058, China. Tel.: +86-571-88206592; Fax: +86-571-85128776; E-mail: wjfu@zju.edu.cn
**These authors contributed equally to this study.

and adipocytes, under corresponding induction media (Jaiswal *et al*. 1997; Mackay *et al*. 1998; Pittenger *et al*. 1999; Jiang *et al*. 2002). Thus, hMSCs represent an ideal source for cell therapies due to their ease of purification, amplification and of their multipotency (Jiang *et al*. 2002; Deans & Moseley 2000). Furthermore, their use involves no particular ethical nor immunological problems for autologous use (Caplan 1991; Prockop 1997; Caplan & Bruder 2001). hMSCs have long been utilized in clinical trials with promising results in the areas of cell therapy and tissue engineering, particularly for their use as a source of regenerating cells as vehicles for local gene delivery in genetic and acquired diseases (Wakitani *et al*. 1995; Dennis & Caplan 1996; Javazon *et al*. 2001; Gimeno *et al*. 2005; Bernardo *et al*. 2006).

However, hMSCs isolated from human bone marrow have a limited lifespan (Stenderup *et al*. 2003); they enter cell senescence and cease dividing after several cell divisions in *ex vivo* culture (Hayflick 1976; Campisi 1997; Shi *et al*. 2002; Simonsen *et al*. 2002; Qiu *et al*. 2004). Telomerase reverse transcriptase (TERT) is able to immortalize cells, and Shi *et al*. (2002) and Simonsen *et al*. (2002) forced expression of telomerase to extend replicative capacity of hMSCs. hMSCs transduced with hTERT retained their functional characteristics and differentiation potential, and on transplantation into immunodeficient mice they formed bone tissue more effectively than non-transduced cells (Simonsen *et al*. 2002). However, Burns *et al*. (2005) and Simonsen *et al*. (2002) also found the neoplastic potential of some hTERT-transduced hMSC lines at different population doubling levels. We also have established a line of hMSCs transduced with hTERT (hTERT–hMSCs) and cultured these cells for more than 290 population doublings (PDs) without loss of contact inhibition (Huang *et al*. 2007).

The science of proteomics provides a systematic approach for qualitative and quantitative mapping of cells' whole proteome. The proteome is the cell-specific protein complement from the genome and encompasses all proteins that are expressed in a cell in a particular condition. Effects of exogenous hTERT on proliferation of hMSCs can be reflected through changes in the proteome. In this study, we used two-dimensional gel electrophoresis (2-DE) to establish proteomic patterns of primary hMSCs and hTERT–hMSCs as well as to monitor sustaining of protein expression in hTERT–hMSCs during proliferation. Finally, the expression pattern of key proteins and their roles in proliferation of hTERT–hMSCs is discussed. Our results provide a preliminary insight into global response of hMSCs after transduction with hTERT.

## MATERIALS AND METHODS

### Cell culture

Human bone marrow samples were collected from healthy human donors (18–46 years old) under a protocol approved by the Institutional Review Board. Each sample was washed twice with phosphate-buffered saline (PBS) and being suspended. The cell suspension was centrifuged over a Ficoll step gradient with a density of 1.077 g/mL (Ficoll-Histopaque 1077, Sigma, Shanghai, China) at 1800 ***g*** for 20 min. The mononuclear cell layer at the Ficoll/plasma interface was aspirated, washed twice with PBS, and then suspended in hMSCs medium in a flask at a density of $2 \times 10^7$ cells per 75 $cm^2$. Cells were cultured at 37 °C in 95% air–5% $CO_2$ atmosphere. hMSCs medium consisted of minimal essential medium α (HyClone, Shanghai, China) supplemented with 10% (v/v) foetal bovine serum (FBS; Gibco-BRL, Hangzhou, China) and 1% antibiotic solution (Life Technologies, Beijing, China). In 14 days, the well-spread and attached hMSCs reached 90% confluence. After removal of non-adherent cells by changing the medium, hMSCs were detached using trypsin-EDTA (Life Technologies) and were seeded in a flask at a density

of $5 \times 10^5$ cells per 75 $cm^2$ as passage 1. At confluence of 70–90%, cells were harvested and diluted 1 : 3 for passage. Cells at passage 3 showed surface antigen phenotypes of hMSCs (Xiang *et al*. 2007).

Human mesenchymal stem cells at passage 3 were transduced using retroviruses constructed with hTERT as previously described (Huang *et al*. 2007). Briefly, the retroviral vector pHy-hTERT was constructed by subcloning hTERT cDNA from pGRN145 into pHy (between Hpa I and Not I sites) and was transduced into the packaging cell line PA317, to produce viral supernatant using Lipofectamine™ Transfection Reagent (Life Technologies). Transduced cells were selected with 200 μg/mL hygromycin for 7 days. Titres of pHy-hTERT-derived retroviruses were analysed using NIH-3T3 target cells with varied dilutions of retroviral supernatants. Primary hMSCs ($2.0 \times 10^5$) at passage 3 in a 10-cm dish were exposed to viral supernatant containing retrovirus at an approximate multiplicity of infection of 300, for 8 h in the presence of 8 μg/mL polybrene (Sigma, Hangzhou, China). Transduced cells were washed twice with PBS and were incubated for 48 h, then selected with 20 μg/mL hygromycin for 7 days. Surviving cells were then cloned using a limited dilution method (Zhu *et al*. 2007); these were noted as first passage of hTERT–hMSCs. The cells were cultured in minimal essential medium α (HyClone) supplemented with 10% FBS, 100 μg/mL penicillin and streptomycin (Sigma, Hangzhou, China) at 37 °C in a humidified atmosphere with 5% $CO_2$. Medium was changed thrice a week. When reaching 70% confluence, the cells from each clone were trypsinized with 0.25% trypsin-EDTA (Sigma, Hangzhou, China) and diluted 1 : 2 for passage.

For each passage, cells from subconfluent cultures were counted using a haemocytometer. PDs were calculated using the formula: PD = log[(*n* cells in)/(*n* cells out)]/log2 (Burns *et al*. 2005). PD time was calculated from the average of two consecutive passages.

**Sample preparation and 2-DE analysis**

Primary hMSCs at PD 12 and hTERT–hMSCs cells at PD 95 and PD 275 were harvested, and then washed in cold PBS before being centrifuged at 800 ***g*** for 10 min at 4 °C, four times; pellets were stored at –80 °C before protein lysis. Cells ($2–3 \times 10^6$) were dissolved in a detergent lysis buffer containing 8 M urea, 2 M thiourea, 4% (w/v) 3-[(3-Cholamidopropyl)dimethyl-ammonio]-1-propanesulfonate (CHAPS), 0.5% (v/v) Triton X-100, 0.5% (v/v) immobilization pH gradient (IPG) buffer pH 3–10 or pH 4–9 (Amersham Biosciences, Shanghai, China), 100 mM dithriothreitol, and 1.5 mg/mL complete protease inhibitor (Roche, Shanghai, China) for 1 h at 18 °C in an orbital shaker. The lysate was then centrifuged at 21 000 ***g*** for 30 min and protein content in the supernatant was measured by the Bradford assay (Ramagli 1999). Protein extracts were separated using 2-DE, according to the method described previously, with some modifications (Gorg *et al*. 2000; Feldmann *et al*. 2005). Briefly, for isoelectric focusing (first dimension), 500 μg of protein lysate were run in 6 M urea, 2 M thiourea, 1 M dithriothreitol, 2% (w/v) CHAPS, and 0.5% (v/v) IPG buffer on 18-cm immobilized non-linear pH 3–10 or pH 4–9 gradient IPG strips in the IPGphor apparatus (Amersham Biosciences) using the following protocol: after 12 h re-swelling time at 30 V, voltages of 200 V, 500 V and 1000 V were applied for 1 h each. Then, voltage was increased to 8000 V within 30 min and kept constant at 8000 V for another 12 h, resulting in a total of 100 300 Vh. For the subsequent sodium dodecyl sulphate-polyacrylamide gel electrophoresis (SDS-PAGE; second dimension), proteins were transferred to $20 \times 18 \times 0.4$ $cm^3$ polyacrylamide gels and were separated by their mass in a 12.5% acrylamide matrix. Protein spots in three different experiments (replicate gels) were visualized by silver staining (Shevchenko *et al*. 1996) and were scanned with an image scanner (GS-800 calibrated densitometry, Bio-Rad, Hercules, CA, USA). Software of PD-Quest 7.2 (Bio-Rad) was employed for image analysis, including background subtraction, spot detection, volume normalization and matching. A reference gel

containing all spots detected on any gel was established. Average gels were matched to the reference gel, and the average gels derived from hTERT–hMSCs at PD 95 and PD 275, and primary hMSCs groups were compared. For each protein spot, significant differences were assessed *via* unpaired Student's *t*-tests using SPSS 12.0 for Windows (SPSS Inc., Chicago, IL, USA). The thresholds were defined as a significant change in spot volume being at least 2-fold or the $P$ value < 0.05 on the comparison to average gels between hTERT–hMSCs and primary hMSCs. Differentially expressed protein spots were selected for further identification by matrix-assisted laser desorption/ionization time-of-flight mass spectrometry (MALDI-TOF-MS).

**Protein identification by mass spectrometry**

Protein identification was achieved by peptide mass fingerprinting (PMF) using MALDI-TOF-MS and gel matching *via* polynomial image warping. For MALDI-TOF-MS, protein spots were automatically located, excised and de-stained (Gharahdaghi *et al*. 1999), and in-gel digestion with trypsin (Promega, Shanghai, China) was employed (Vogt *et al*. 2003). Samples were prepared using α-cyano-4-hydroxy-cinnamic acid as matrix, loaded on to pre-spotted AnchorChip targets (Feldmann *et al*. 2005), and were allowed to air dry at room temperature. Peptide mass spectra were obtained using an Ultraflex TOF/TOF (Bruker Daltonics, Beijing, China) in the fully automated reflectron TOF operation mode controlled by FlexControl software (Bruker Daltonics, Billerica, MA, USA) (Feldmann *et al*. 2005). The parameters of MALDI-TOF were set up as follows: 20 kV accelerating voltage, 65% grid voltage, 100–120 ns delay time and acquisition mass range 900–3500 Da. Spectra were accumulated from 100 laser shots and were internally calibrated using autolytic fragments of trypsin. Obtained PMF were searched in the Swiss-Prot database using Mascot software (http://www.matrixscience.com) with the following parameters: taxonomy selected as *Homo sapiens* (human); mass tolerance ±75 p.p.m.; missed cleavage sites allowed up to 1; fixed modification selected as carbamidomethylation (cysteine) and variable modification selected as oxidation (methionine). Probability scores calculated by software were used as criteria for correct identification (Perkins *et al*. 1999; Maurer *et al*. 2004; Feldmann *et al*. 2005). Three analytical gels were performed for each group.

**Semiquantitative reverse transcriptase–polymerase chain reaction**

Total RNA was isolated from the primary hMSCs at PD 12, hTERT–hMSCs at PD 95 and PD 275, using TRIzol reagent (Invitrogen Life Technologies, Beijing, China). First strand cDNA was generated using the SuperScript First-Strand Synthesis System (Invitrogen Life Technologies) according to the manufacturer's protocol. Polymerase chain reaction (PCR) was performed using 1 μL total cDNA mixed with 1× PCR buffer, 1.5 μM $MgCl_2$, 0.2 μM deoxynucleoside triphosphate (dNTP) and 1 μM of one of the following gene-specific oligonucleotide primer pairs: annexin A1, forward: 5′-CATATCTCCAGGAAACAGGA-3′ and reverse: 5′-ATCTCCAGATGTGTCTGAGG-3′; annexin A2, forward: 5′-AACCGACGAGGACTCTCTCA-3′ and reverse: 5′-GCTGATCCACTTGGGAA-CAT-3′; annexin V, forward: 5′-CTGCCTACCTTGCAGAGACC-3′ and reverse: 5′-CTTCCCCGT-GACACGTTAGT-3′; glutathione S-transferase P1 (GSTP1), forward: 5′-GGCAACTGAAG-CCTTTTGAG-3′ and reverse: 5′-GGCTAGGACCTCATGGATCA-3′; reticulocalbin 1 (RCN1), forward: 5′-GGAGTTCACTGCCTTTCTGC-3′ and reverse: 5′-ATCCAGTGGCGAATCTCATC-3′; chaperonin-containing T-complex subunit-6 (CCT6A), forward: 5′-TGGGACATGCAGGACTTGTA-3′ and reverse: 5′-AACCACACAGCCATCATCAA-3′; actin γ1 propeptide (ACTG1), forward: 5′-TCTGTGGCTTGGTGAGTCTG-3′ and reverse: 5′-AGTAACAGCCCACGGTGTTC-3′; tubulin α1b (TUBA1B), forward: 5′-ATGGAGCCCTGAATGTTGAC-3′ and reverse: 5′-CTCAAAGCAAGCATTGGTGA-3′; p53, forward: 5′-GGCCCACTTCACCGTACTAA-3′ and reverse: 5′-GTGGTTTCAAGGCCAGATGT-3′; prohibitin (PHB), forward: 5′-GGCTGAGCAACA-

 

GAAAAAGG-3′ and reverse: 5′-GCTGGCAGGTAGGTGATGTT-3′; and glyceraldehyde 3-phosphate dehydrogenase (GAPDH), forward: 5′-CCAGAACATCATCCCTGCCTCTAC-3′ and reverse: 5′-GGTCTCTCTCTTCCTCTTGTGC-3′. PCR amplifications were performed using the following conditions: after 5 min denaturation at 94 °C, 32 cycles of PCR were performed with each cycle including denaturation at 95 °C (15 s), annealing at 59 °C (annexin A1, 45 s), 55 °C (annexin A2, 40 s), 54 °C (annexin V, 45 s), 56 °C (GSTP1, 40 s), 54 °C (RCN1, 45 s); 53 °C (CCT6A, 45 s), 56 °C (ACTG1, 40 s), 58 °C (TUBA1B, 40 s), 53 °C (p53, 45 s), 54 °C (prohibitin, 45 s), 58 °C (GAPDH, 40 s) and primer extension at 72 °C (90 s). A final extension was carried out for 5 min and stopped at 4 °C. PCR products were visualized after electrophoresis on 1.5% agarose gel and ethidium bromide staining. The expected product sizes were 278 bp (annexin A1), 280 bp (annexin A2), 236 bp (annexin V), 128 bp (GSTP1), 252 bp (RCN1), 194 bp (CCT6A), 210 bp (ACTG1), 158 bp (TUBA1B), 156 bp (p53), 158 bp (prohibitin) and 450 bp (GAPDH). Intensity of the bands was determined using AlphaEase software (Alpha Innotech, Beijing, China) and normalized to band intensity for GAPDH. Each experiment was repeated three times.

### Western blot analysis

Western blot analysis was performed to measure protein expression of annexin A1, annexin A2, annexin V, GSTP1, reticulocalbin 1, CCT6A, ACTG1, TUBA1B, p53 and prohibitin. Cells were washed twice with PBS and proteins were obtained using NE-PER Nuclear and Cytoplasmic Extraction Reagents (Pierce, Beijing, China). Fifty micrograms of protein extracts were separated on a 12.5% SDS-PAGE and were transferred to nitrocellulose membranes. Mouse antireticulocalbin 1 (Jinmei Biotech, Hangzhou, China), mouse anti-annexins A1, A2 and V (Chemicon, Hangzhou, China), mouse anti-GSTP1, mouse anti-CCT6A (Chemicon), mouse anti-ACTG1, mouse anti-TUBA1B (Sigma, Hangzhou, China), mouse antip53 (Jinmei Biotech) and mouse antiprohibitin (Jinmei Biotech) were used as the primary antibodies. Horseradish peroxidase-conjugated secondary antibodies were purchased from Amersham Pharmacia Biotech (Hong Kong, China). Anti-GAPDH monoclonal antibody was purchased from Sigma. Proteins were visualized by means of enhanced chemiluminescence (Sigma, Hangzhou, China). Intensity of the bands was determined using AlphaEase software (Alpha Innotech) and was normalized to band intensity for anti-GAPDH and semiquantitatively analysed using the software package ImageMaster software (GE Healthcare Biosciences, Uppsala, Sweden). Each experiment was repeated three times.

### Statistical analysis

Statistical significance between groups was determined using mean ± SEM, and statistical comparisons were performed using the Student's *t*-test. A level of $P < 0.05$ was accepted as significant.

## RESULTS

### Protein expression profiles of primary hMSCs and hTERT–hMSCs

A line of hMSCs transduced with exogenous hTERT (hTERT–hMSCs) was established and cultured for 290 PDs, about 1056 days, without loss of contact inhibition (Huang *et al*. 2007). The exogenous *hTERT* gene is stably expressed in hMSCs (Fig. 1). Flow cytometry analysis demonstrated that hTERT–hMSCs maintained identical properties of cell surface antigens as

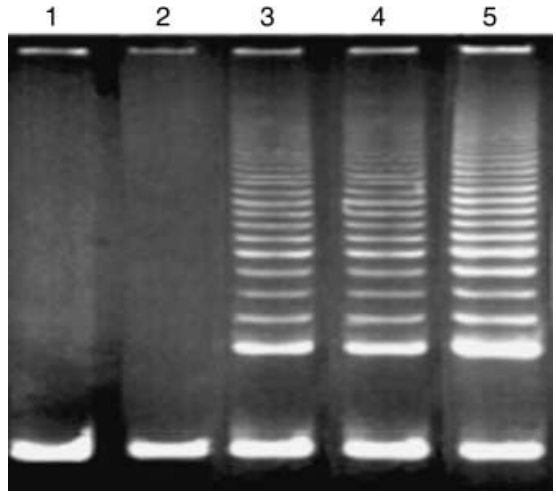


**Figure 1. Telomerase activity was analysed by telomeric repeat amplification protocol assay**. No telomerase activity was detected in the primary hMSCs at PD 12 (lane 1) and the CHAPS buffer alone (lane 2). hTERT–hMSCs cells at PD 95 or 275 exhibited significant telomerase activity (lanes 3 and 4, respectively) compared with that of the NIH-3T3 cells (lane 5), positive control. hMSCs, human mesenchymal stem cells; hTERT, human telomerase reverse transcriptase.

primary hMSCs, that is, expression of CD29, CD44, CD105 and CD166, and lack of expression of CD34, CD45, CD117 and HLA-DR. Under adipogenic, chondrogenic and osteogenic induction, hTERT–hMSCs at PD 95 and PD 275, respectively, could still differentiate into adipocytes, chondrocytes and osteocytes. However, hTERT–hMSCs at these PDs showed no transforming activity through both *in vitro* assay of cell growth in soft agar and *in vivo* assay of tumorigenicity in non-obese diabetic/severely compromised immunodeficient mice. Karyotype analyses also showed no significant chromosomal abnormalities in the hTERT–hMSCs at these PDs (Huang *et al*. 2007).

For comparison of protein expression profiles of hTERT–hMSCs with that of primary hMSCs, differential protein expressions in primary hMSCs at PD 12, hTERT–hMSCs at PD 95 and at PD 275 were evaluated using 2-DE analyses of total protein extracts. In the first dimension, we used a wide pH interval of 3–10 for IPG strips to view total protein distributions. The wide-range 2-DE maps showed that most protein spots were located in the middle region of the gel. Then, IPG strips with the narrower pH range of 4–9 were used to achieve better separation of these middle gel part protein spots. After three procedure cycles, three pieces of two-dimensional gels were obtained, respectively, from primary hMSCs at PD 12, hTERT–hMSCs at PD 95 and hTERT–hMSCs at PD 275. Images of silver-stained two-dimensional gels were photographed with GS-800 calibrated densitometry and were analysed by PD-Quest software. Matching analyses showed that matching ratios of these gel images reached 90.5% for primary MSCs, 88.4% for hTERT–hMSCs at PD 95 and 89.3% for hTERT–hMSCs at PD 275, which indicated perfect reproducibility of these images. Representative 2-DE maps for primary MSCs at PD 12, hTERT–hMSCs at PD 95 and hTERT–hMSCs at PD 275 are shown in Fig. 2a–c. According to the analysis of 2-DE analytical gels after automatic spot detection, background subtraction and volume normalization, $1543 \pm 145$ protein spots in gels of primary MSCs, $1611 \pm 186$ protein spots in gels of hTERT–hMSCs at PD 95 and $1451 \pm 126$ protein spots in gels of hTERT–hMSCs at PD 275 were detected.

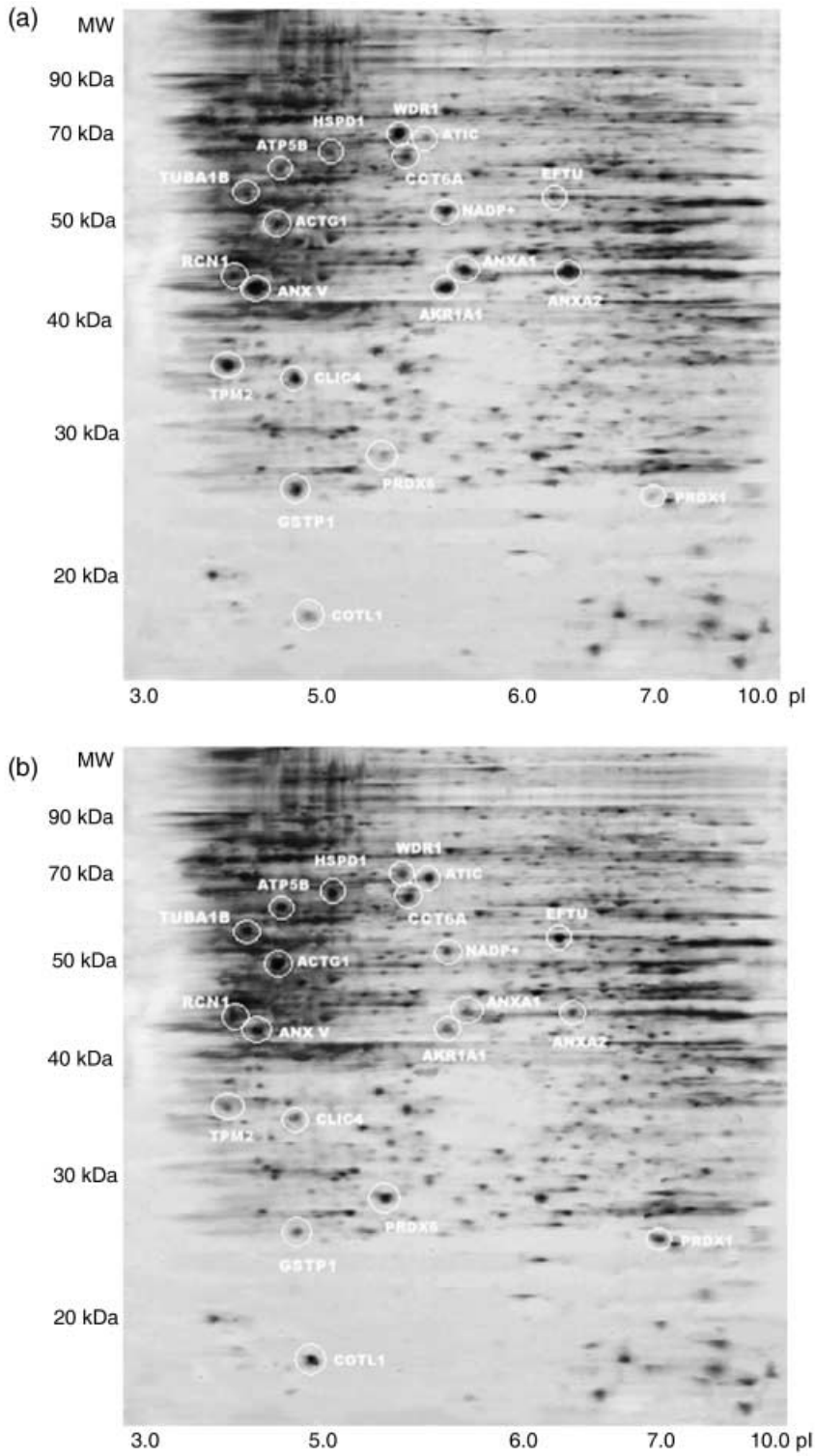

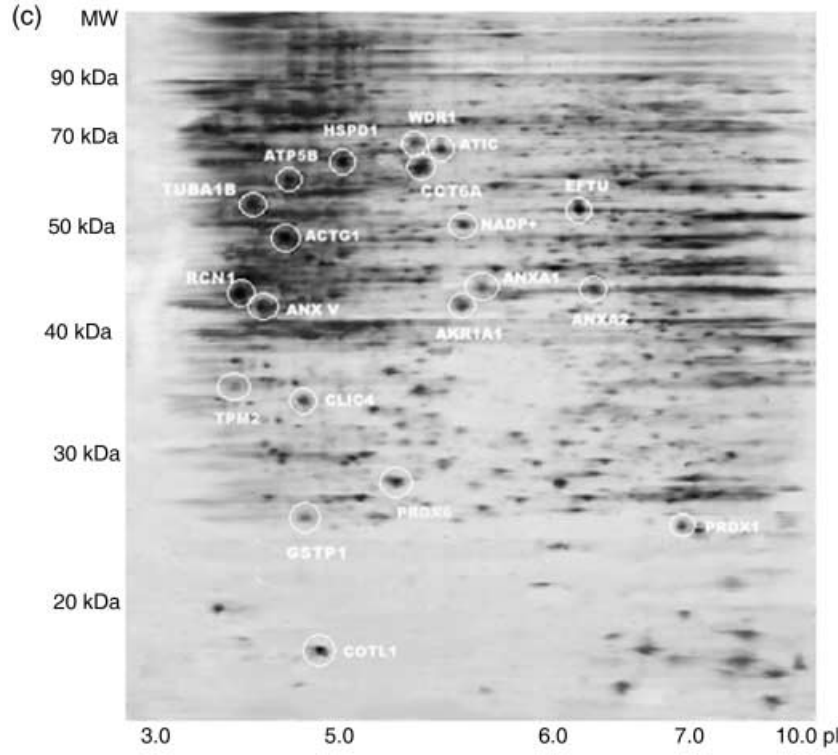


**Figure 2. Representative 2-DE protein profiles from primary human MSCs at PD 12 (a), hTERT-hMSCs at PD 95 (b) and hTERT–hMSCs at PD 275 (c).** Proteins were separated on the basis of isoelectric point (X-axis) and molecular mass (Y-axis) and visualized by silver staining. Twenty differential expression protein spots were identified and are marked with circles. hMSCs, human mesenchymal stem cells; hTERT, human telomerase reverse transcriptase.

### Protein identification by peptide mass fingerprinting analysis

According to the comparison of protein profiles from primary hMSCs at PD 12, hTERT–hMSCs at PD 95 and PD 275 by PD-Quest two-dimensional software, we chose 100 protein spots for protein identification by PMF, using MALDI-TOF-MS. Subsequent bio-informatic data were searched in the National Center for Biotechnology Information (NCBI) database by using Mascot software (Matrix Science, London, UK) to identify the proteins. All the 100 identified proteins are listed in Table 1. Only Mascot database query results that were statistically significant at the 5% level were considered. Three analytical gels were performed for each group. Of spots analyzed, 12 protein spots showed up-regulation in hTERT-hMSCs at PD 95 and PD 275 by comparing with those of primary MSCs ($P < 0.05$). These proteins were chaperonin containing T-complex subunit 6 (CCT6A), Reticulocalbin 1 (RCN 1), glutathione S-transferase P 1 (GSTP1), tubulin α1b (TUBA1B), actin γ1 propeptide (ACTG1), IMP cyclohydrolase (ATIC), ATP synthase F1 complex (ATP5B), peroxiredoxin 6 (PRDX6), peroxiredoxin 1 (PRDX1), elongation factor TU (EFTU), coactosin-like 1 (COTL1) and heat shock 60 kDa 1 (HSPD1). 8 protein spots showed down-regulation in hTERT-hMSCs at PD 95 and PD 275 by comparing with those of primary MSCs ($P < 0.05$). These proteins were β tropomyosin (TPM2), WD repeat

 

**Table 1.** All 100 identified proteins, along with their respective database accession information

| Spot no. | NCBI Entrez Protein annotation | NCBI Entrez Protein accession | Swiss-Prot Protein accession | Molecular weight (MW) (Da) | Isoelectric point (pI) | Score | Peptides matched | Peptides obtained | Sequence coverage (%) |
|---|---|---|---|---|---|---|---|---|---|
| 1 | Actin, γ1 propeptide; cytoskeletal γ-actin | gi\|4501887 | P63261 | 42 108 | 5.31 | 159 | 11 | 16 | 35 |
| 2 | Reticulocalbin 1 (RCN1) | gi\|4506455 | Q15293 | 38.890 | 4.86 | 124 | 11 | 24 | 44 |
| 3 | Actin-related protein | gi\|381964 | P42025 | 42 659 | 5.98 | 68 | 12 | 18 | 56 |
| 4 | F-actin capping protein beta subunit (CapZ beta) | gi\|13124696 | P47756 | 31 616 | 5.36 | 112 | 8 | 14 | 32 |
| 5 | ACTB protein | gi\|15277503 | Q96E67 | 40 536 | 5.55 | 135 | 9 | 13 | 25 |
| 6 | Actinin, α1 | gi\|30583253 | P12814 | 103 563 | 5.1 | 92 | 15 | 19 | 45 |
| 7 | Adenylyl cyclase-associated protein | gi\|30583143 | Q01518 | 51 926 | 8.12 | 203 | 14 | 20 | 23 |
| 8 | Alanyl-tRNA synthetase | gi\|4501841 | P49588 | 107 476 | 5.31 | 210 | 20 | 32 | 65 |
| 9 | Aldehyde dehydrogenase 1 family, member B1 | gi\|30583675 | Q9BV45 | 57 658 | 6.36 | 85 | 9 | 17 | 35 |
| 10 | Aldo-keto reductase family 1, member A1 | gi\|24497577 | P14550 | 36 892 | 6.35 | 121 | 7 | 13 | 45 |
| 11 | Aldolase A; fructose-bisphosphate aldolase; Aldolase A | gi\|4557305 | P04075 | 39 851 | 8.39 | 157 | 15 | 27 | 26 |
| 12 | Annexin I; annexin I (lipocortin I); lipocortin I | gi\|4502101 | P04083 | 38 918 | 6.64 | 122 | 15 | 26 | 41 |
| 13 | Annexin A2/ANXA2 | gi\|18645167 | Q8TBV2 | 38 780 | 7.57 | 204 | 13 | 23 | 65 |
| 14 | Annexin 5; lipocortin V; placental anticoagulant protein I | gi\|4502107 | P08758 | 35 971 | 4.94 | 135 | 15 | 24 | 68 |
| 15 | Aspartate aminotransferase 1 | gi\|4504067 | P17174 | 46 447 | 7.1 | 95 | 18 | 32 | 54 |
| 16 | ATPase, $H^+$ transporting, lysosomal 56/58 kDa, V1 subunit B, isoform 2 | gi\|21040528 | P21281 | 56 735 | 5.57 | 76 | 19 | 33 | 35 |
| 17 | ATP synthase, F1 complex/ATP5B | gi\|32189394 | P06576 | 56 525 | 5.26 | 155 | 20 | 26 | 66 |
| 18 | Aargo selection protein/TIP47 | gi\|20127486 | O60664 | 47 189 | 5.3 | 134 | 21 | 32 | 42 |
| 19 | Ahloride intracellular channel 4/CLIC4 | gi\|7330335 | Q9Y696 | 28 982 | 5.45 | 125 | 18 | 25 | 33 |
| 20 | Ahaperonin containing T-complex subunit 6 | gi\|4502643 | P40227 | 58 444 | 6.25 | 175 | 14 | 20 | 46 |
| 21 | Collagen; type VI; α1 precursor | gi\|30851190 | Q7Z645 | 109 602 | 5.26 | 200 | 15 | 19 | 24 |
| 22 | Coactosin-like 1/COTL1 | gi\|21624607 | Q14019 | 16 049 | 5.54 | 78 | 16 | 21 | 29 |
| 23 | Cytosol aminopeptidase (LAP) | gi\|12643394 | P28838 | 53 137 | 6.29 | 114 | 14 | 19 | 24 |
| 24 | Cytosolic malate dehydrogenase | gi\|5174539 | P40925 | 36 631 | 6.89 | 112 | 16 | 19 | 36 |
| 25 | Electron transfer flavoprotein, alpha polypeptide | gi\|4503607 | P13804 | 35 400 | 8.6 | 145 | 18 | 30 | 46 |
| 26 | Elongation factor EF-Tu | gi\|2136315 | P49411 | 49 851 | 7.26 | 124 | 19 | 26 | 54 |
| 27 | Enolase 1/ENO1 | gi\|4503571 | P06733 | 47 481 | 5.78 | 102 | 9 | 15 | 55 |
| 28 | Endoplasmic reticulum protein 29 precursor | gi\|5803013 | P30040 | 29 032 | 6.77 | 142 | 19 | 26 | 35 |
| 29 | Esterase D/formylglutathione hydrolase | gi\|33413400 | P10768 | 31 956 | 6.54 | 201 | 8 | 13 | 61 |
| 30 | Eukaryotic translation elongation factor 2 | gi\|4503483 | P13639 | 96 246 | 6.42 | 98 | 7 | 14 | 31 |
| 31 | Eukaryotic translation initiation factor 5A | gi\|54673799 | P63241 | 17 049 | 4.9 | 157 | 18 | 21 | 28 |

 *Cell Proliferation*, **41**, 625–644.

**Table 1.** *Continued.*

| Spot no. | NCBI Entrez Protein annotation | NCBI Entrez Protein accession | Swiss-Prot Protein accession | Molecular weight (MW) (Da) | Isoelectric point (pI) | Score | Peptides matched | Peptides obtained | Sequence coverage (%) |
|---|---|---|---|---|---|---|---|---|---|
| 32 | Far upstream element binding protein 1 (FUSE binding protein 1) | gi\|37078490 | Q96AE4 | 67 602 | 7.18 | 126 | 17 | 30 | 26 |
| 33 | GDP dissociation inhibitor 2; rab GDP-dissociation inhibitor; beta | gi\|6598323 | P50395 | 51 087 | 6.11 | 134 | 15 | 23 | 29 |
| 34 | Guanine monophosphate synthetase | gi\|4504035 | P49915 | 77 408 | 6.42 | 254 | 13 | 20 | 27 |
| 35 | Glutathione S-transferase omega 1 | gi\|4758484 | P78417 | 27 833 | 6.24 | 142 | 9 | 14 | 35 |
| 36 | Glutathione S-transferase | gi\|2204207 | P09211 | 23 595 | 5.44 | 89 | 8 | 12 | 32 |
| 37 | Glucose regulated protein 58 kDa | gi\|21361657 | P30101 | 57 146 | 5.98 | 134 | 16 | 24 | 29 |
| 38 | Glucosidase II/GANAB | gi\|2274968 | Q14697 | 107 289 | 5.71 | 165 | 15 | 24 | 34 |
| 39 | Glutathione S-transferase/GSTP1 | gi\|2204207 | P09211 | 23 595 | 5.44 | 145 | 17 | 23 | 28 |
| 40 | Glutathione synthetase/GSS | gi\|4504169 | P48637 | 52 523 | 5.67 | 75 | 13 | 19 | 54 |
| 41 | Heat shock 90 kDa protein 1, alpha | gi\|40254816 | P07900 | 85 020 | 4.94 | 123 | 11 | 17 | 28 |
| 42 | Heat shock 90 kDa protein 1, beta | gi\|20149594 | P08238 | 83 554 | 4.7 | 169 | 10 | 16 | 65 |
| 43 | heat shock 70 kDa protein 9B (mortalin-2) | gi\|21040386 | Q8N1C8 | 74 093 | 6.04 | 156 | 10 | 14 | 27 |
| 44 | Prohibitin (PHB, p32) | gi\|4505773 | P35232 | 29 800 | 5.6 | 102 | 8 | 11 | 52 |
| 45 | Heat shock 70 kDa 1/HSPA1A | gi\|462325 | P08107 | 70 294 | 5.48 | 203 | 19 | 26 | 42 |
| 46 | Heat shock 70 kDa 4a/HSP70-4 | gi\|38327039 | P34932 | 95 127 | 5.18 | 205 | 21 | 30 | 44 |
| 47 | Heat shock 70 kDa 5/HSPA5 | gi\|16507237 | P11021 | 72 402 | 5.07 | 142 | 18 | 28 | 65 |
| 48 | Heat shock 70 kDa 8/HSPA8 | gi\|5729877 | P11142 | 71 082 | 5.37 | 76 | 11 | 27 | 39 |
| 49 | Heat shock 60 kDa 1/HSPD1 | gi\|31542947 | P10809 | 61 187 | 5.7 | 198 | 10 | 16 | 37 |
| 50 | Histamine-releasing factor/TPT1 | gi\|4507669 | P13693 | 19 697 | 4.84 | 186 | 8 | 12 | 41 |
| 51 | Isocitrate dehydrogenase 1/IDH1 | gi\|28178825 | O75874 | 46 915 | 6.53 | 125 | 8 | 14 | 33 |
| 52 | IMMT | gi\|48145703 | Q6IBL0 | 84 027 | 6.08 | 169 | 9 | 13 | 29 |
| 53 | IMP cyclohydrolase/ATIC | gi\|20127454 | P31939 | 65 089 | 6.27 | 154 | 12 | 19 | 22 |
| 54 | Laminin-binding protein/LAMR1 | gi\|34234 | P08865 | 31 888 | 4.79 | 156 | 18 | 24 | 54 |
| 55 | Lactate dehydrogenase B/LDHB | gi\|4557032 | P07195 | 36 900 | 5.72 | 98 | 17 | 23 | 27 |
| 56 | Microtubule-associated protein, RP/EB family, member 1 | gi\|6912494 | Q15691 | 30 151 | 5.02 | 86 | 14 | 26 | 52 |
| 57 | Mitochondrial short-chain enoyl-coenzyme A hydratase 1 precursor | gi\|12707570 | P30084 | 31 807 | 8.34 | 168 | 11 | 20 | 69 |
| 58 | Major vault protein/MVP | gi\|19913410 | Q14764 | 99 551 | 5.34 | 137 | 13 | 16 | 28 |
| 59 | NADH dehydrogenase (ubiquinone) Fe-S protein 1, 75 kDa precursor | gi\|33519475 | P28331 | 80 443 | 6.2 | 169 | 14 | 18 | 70 |
| 60 | Neuropolypeptide h3, prostatic binding protein | gi\|913159 | P30086 | 21 027 | 7.43 | 173 | 12 | 19 | 56 |
| 61 | Peroxiredoxin 6 | gi\|28559000 | P30041 | 25.133 | 6.02 | 123 | 11 | 18 | 56 |
| 62 | peroxiredoxin 1 (PRDX1) | gi\|4505591 | Q06830 | 22.3 | 8.27 | 154 | 15 | 19 | 68 |
| 63 | Phosphoprotein phosphatase 2-alpha 65K regulatory chain | gi\|107300 | P30153 | 65 980 | 4.96 | 179 | 7 | 10 | 28 |

 

| | | | | | | | | | |
|---|---|---|---|---|---|---|---|---|---|
| 64 | Pyruvate kinase 3 isoform 1 | gi\|33286418 | P14618 | 58 470 | 7.95 | 175 | 19 | 28 | 36 |
| 65 | 3-Phosphoglycerate dehydrogenase | gi\|2674062 | O43175 | 57 370 | 6.31 | 143 | 23 | 29 | 62 |
| 66 | PRP19/PSO4 homolog | gi\|7657381 | Q9UMS4 | 55 603 | 6.14 | 78 | 21 | 32 | 36 |
| 67 | Poly(rC) binding protein 1 | gi\|5453854 | Q15365 | 38 015 | 6.66 | 149 | 8 | 16 | 35 |
| 68 | Procollagen-lysine/PLOD2 | gi\|4505889 | O00469 | 85 351 | 6.15 | 155 | 15 | 19 | 34 |
| 69 | Pyrroline-5-carboxylate reductase 1 isoform 2 | gi\|24797095 | Q96C36 | 33 548 | 7.66 | 201 | 16 | 20 | 33 |
| 70 | Phosphoglycerate mutase 1 (brain) | gi\|38566176 | P18669 | 28 916 | 6.67 | 213 | 12 | 19 | 26 |
| 71 | 6-Phosphogluconolactonase | gi\|6912586 | O95336 | 27 815 | 5.70 | 67 | 21 | 32 | 28 |
| 72 | Proteasome alpha 2 subunit | gi\|4506181 | P25787 | 25 996 | 7.12 | 144 | 21 | 34 | 27 |
| 73 | Phosphoserine aminotransferase | gi\|25140375 | Q9Y617 | 40 796 | 7.56 | 178 | 14 | 23 | 35 |
| 74 | Prolyl 4-hydroxylase/P4HB | gi\|20070125 | P07237 | 57 480 | 4.76 | 136 | 12 | 25 | 26 |
| 75 | Plastin 3 | gi\|7549809 | P13797 | 71 279 | 5.52 | 147 | 11 | 20 | 24 |
| 76 | Peptidylprolyl isomerase A/PPIA | gi\|10863927 | P05092 | 18 229 | 7.82 | 159 | 10 | 14 | 55 |
| 77 | RuvB-like 1, TATA binding protein interacting protein 49 kDa | gi\|4506753 | Q9Y265 | 50 538 | 6.02 | 176 | 7 | 12 | 26 |
| 78 | Actinin, α1/ACTN1 | gi\|30583253 | P12814 | 103 563 | 5.22 | 81 | 9 | 22 | 13 |
| 79 | RNA-binding protein regulatory subunit; oncogene DJ1 | gi\|31543380 | O14805 | 20 050 | 6.33 | 158 | 16 | 21 | 28 |
| 80 | RNA-binding protein/PARK7 | gi\|31543380 | O14805 | 20 050 | 6.33 | 135 | 16 | 24 | 24 |
| 81 | Rho GDP dissociation inhibitor (GDI) | gi\|36038 | P52565 | 23 236 | 5.03 | 145 | 22 | 31 | 26 |
| 82 | Ras-related nuclear protein | gi\|48734884 | P62826 | 24 609 | 7.01 | 169 | 24 | 30 | 28 |
| 83 | 26S proteasome-associated pad1 homolog | gi\|5031981 | O00487 | 34 726 | 6.6 | 157 | 13 | 21 | 34 |
| 84 | Serine/threonine kinase receptor associated protein | gi\|20149592 | Q9Y3F4 | 38 770 | 4.98 | 178 | 11 | 20 | 36 |
| 85 | Spermidine synthase | gi\|21620021 | P19623 | 34 373 | 5.3 | 65 | 10 | 18 | 28 |
| 86 | Transaldolase 1 | gi\|5803187 | P37837 | 37 688 | 6.36 | 135 | 14 | 21 | 24 |
| 87 | Tumour rejection antigen (gp96) 1 | gi\|4507677 | P14625 | 92 696 | 4.76 | 79 | 16 | 20 | 68 |
| 88 | Tyrosyl-tRNA synthetase | gi\|4507947 | P54577 | 59 448 | 6.64 | 135 | 14 | 19 | 56 |
| 89 | Tropomodulin 3 (ubiquitous) | gi\|7657649 | Q9NYL9 | 39 741 | 5.08 | 145 | 13 | 17 | 23 |
| 90 | Tryptophanyl-tRNA synthetase isoform a | gi\|47419916 | P23381 | 53 474 | 6.2 | 69 | 11 | 20 | 35 |
| 91 | Tryptophanyl-tRNA synthetase isoform b | gi\|47419920 | P23381 | 49 163 | 6.5 | 86 | 15 | 18 | 41 |
| 92 | Translation initiation factor eIF-4A2 homolog | gi\|631472 | P38919 | 47 088 | 6.3 | 241 | 19 | 24 | 26 |
| 93 | Transgelin/TAGLN2 | gi\|3123283 | Q01995 | 22 653 | 8.88 | 137 | 17 | 20 | 29 |
| 94 | β-Tropomyosin/TPM2 | gi\|6573280 | P07951 | 29 980 | 4.66 | 186 | 15 | 20 | 43 |
| 95 | Triosephosphate isomerase 1/TPI1 | gi\|4507645 | Q8WWD0 | 26 938 | 6.45 | 196 | 13 | 18 | 35 |
| 96 | Tubulin α/Kα1 | gi\|5174477 | P05209 | 50 804 | 4.94 | 183 | 14 | 24 | 52 |
| 97 | Ubiquinol-cytochr. c red. I/UQCRC1 | gi\|4507841 | P31930 | 53 270 | 5.94 | 174 | 16 | 25 | 27 |
| 98 | Transitional endoplasmic reticulum ATPase | gi\|48257098 | P55072 | 71 534 | 5.14 | 96 | 17 | 24 | 19 |
| 99 | Vinculin isoform/VCL | gi\|4507877 | P18206 | 117 220 | 5.51 | 86 | 9 | 17 | 23 |
| 100 | WD repeat-containing 1/WDR1 | gi\|9257257 | O75083 | 66 836 | 6.17 | 97 | 19 | 23 | 35 |

 

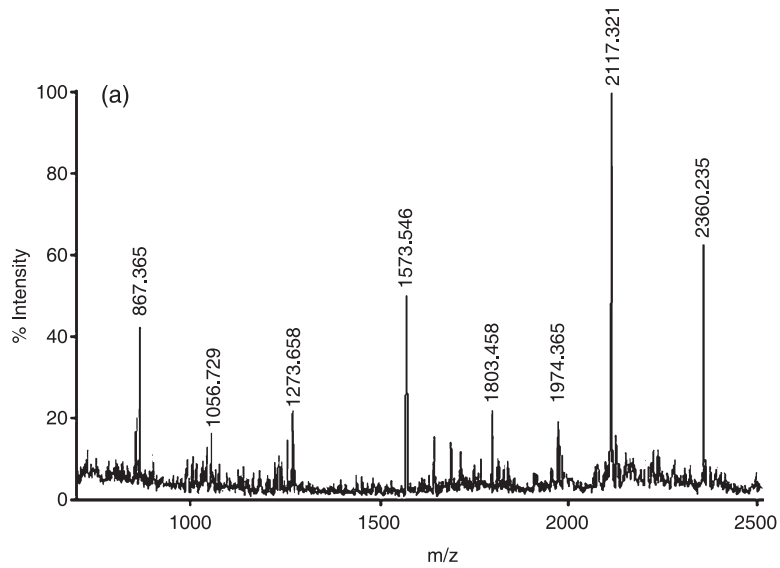


**Figure 3. PMF analysis of differentially expressed proteins with spot 2 as typical protein**. (a) Peptide mass fingerprint for trypsin digest of spot 2 identified as reticulocalbin 1. The X-axis represents mass-to-charge ratio (m/z), whereas the Y-axis represents relative abundance. (b) Protein sequence of reticulocalbin 1 and matched peptide fragments indicated in bold font and underlined. Fixed modifications: carbamidomethyl; variable modifications: oxidation; cleavage by trypsin: cuts C-term side of KR unless next residue is P; number of mass values searched: 24; number of mass values matched: 11; sequence coverage: 44%.

domain 1 (WDR1), chloride intracellular channel 4 (CLIC4), aldo-keto reductase family 1 member A1 (AKR1A1), isocitrate dehydrogenase 1 (NADP+), Annexin V (ANX V), Annexin A1 (ANXA1) and Annexin A2 (ANXA2). The 20 differentially expressed proteins are listed in Table 2. A representative PMF map and database query result of protein spot 2 in primary hMSCs are shown in Fig. 3a and b. This spot was identified to be RCN1 with the top score of 124 and sequence coverage of 44%. However, there were no significant differences of these 20 protein expressions between hTERT–hMSCs at PD 95 and PD 275 ($P > 0.05$). These 20 proteins were involved in cell functions, such as protein folding, protein binding, structural protein, energy generation, transcription translation, antioxidant, signal transduction, intermediary metabolism and $Ca^{2+}$ binding. Figure 4 shows distribution of the 20 proteins according to their biological functions. Although the hTERT protein was not identified by PMF, due to limitation of IPG (pH 4–9) and SDS-PAGE used in our experiments, Fig. 1 showed the difference of hTERT expression between primary hMSCs and hTERT–hMSCs.

**Table 2.** Search results of differently expressed proteins in hTERT-hMSCs in comparison with primary hMSCs

| Spot no. | Reporter identifier | Density volume (hMSC at PD 12) | Density volume (hMSC–hTERT at PD 95) | Density volume (hMSC–hTERT at PD 275) | *P*-value | Expression in hMSC–hTERT | Molecular weight (MW) (Da) | Isoelectric point (pI) | Type |
|---|---|---|---|---|---|---|---|---|---|
| 1 | Actin, γ1 propeptide (ACTG1) | 356 ± 31 | 748 ± 27 | 854 ± 19 | < 0.05 | Up-regulated | 42.08 | 5.3 | Structural protein |
| 2 | Reticulocalbin 1 (RCN1) | 458 ± 29 | 1067 ± 34 | 1878 ± 56 | < 0.01 | Up-regulated | 38.890 | 4.86 | $Ca^{2+}$ binding protein |
| 17 | ATP synthase, F1 complex (ATP5B) | 452 ± 32 | 1401 ± 36 | 1853 ± 73 | < 0.01 | Up-regulated | 56.525 | 5.26 | Energy generation |
| 20 | Chaperonin-containing T-complex subunit 6 (CCT6A) | 585 ± 36 | 1872 ± 67 | 3335 ± 134 | < 0.05 | Up-regulated | 58.444 | 6.25 | Protein folding |
| 22 | Coactosin-like 1 (COTL1) | 420 ± 34 | 1932 ± 35 | 1974 ± 48 | < 0.01 | Up-regulated | 16.049 | 5.54 | Antioxidant |
| 26 | Elongation factor TU (EFTU) | 356 ± 14 | 1602 ± 175 | 1531 ± 95 | < 0.01 | Up-regulated | 49.851 | 7.26 | Transcription translation |
| 49 | Heat shock 60 kDa 1 (HSPD1) | 365 ± 24 | 1095 ± 46 | 1606 ± 45 | < 0.01 | Up-regulated | 61.187 | 5.7 | Protein folding |
| 53 | IMP cyclohydrolase (ATIC) | 542 ± 34 | 1626 ± 56 | 1572 ± 43 | < 0.01 | Up-regulated | 65.089 | 6.27 | Intermediary metabolism |
| 61 | Peroxiredoxin 6 (PRDX6) | 567 ± 56 | 2552 ± 135 | 2324 ± 156 | < 0.05 | Up-regulated | 25.133 | 6.02 | Antioxidant |
| 62 | Peroxiredoxin 1 (PRDX1) | 463 ± 41 | 2417 ± 168 | 2084 ± 201 | < 0.05 | Up-regulated | 22.3 | 8.27 | Antioxidant |
| 96 | Tubulin, alpha 1b (TUBA1B) | 621 ± 26 | 1242 ± 61 | 1428 ± 37 | < 0.01 | Up-regulated | 50.804 | 4.94 | Structural protein |
| 10 | Aldo-keto reductase family 1, member A1 (AKR1A1) | 2431 ± 41 | 729 ± 49 | 972 ± 53 | < 0.01 | Down-regulated | 36.200 | 6.55 | Intermediary metabolism |
| 12 | Annexin A1 (ANXA1) | 4234 ± 289 | 889 ± 51 | 931 ± 27 | < 0.01 | Down-regulated | 38.918 | 6.64 | $Ca^{2+}$ binding protein |
| 13 | Annexin A2 (ANXA2) | 5347 ± 256 | 802 ± 44 | 1016 ± 48 | < 0.01 | Down-regulated | 38.780 | 7.57 | $Ca^{2+}$ binding protein |
| 14 | Annexin V (ANX V) | 5421 ± 356 | 1084 ± 33 | 976 ± 19 | < 0.01 | Down-regulated | 35.971 | 4.94 | $Ca^{2+}$ binding protein |
| 19 | Chloride intracellular channel 4 (CLIC4) | 3452 ± 134 | 518 ± 56 | 828 ± 64 | < 0.01 | Down-regulated | 28.982 | 5.45 | Signal transduction |
| 39 | Glutathione S-transferase P1 (GSTP1) | 1354 ± 123 | 542 ± 12 | 406 ± 17 | < 0.01 | Down-regulated | 23.595 | 5.44 | Protein binding |
| 51 | Isocitrate dehydrogenase 1 ($NADP^+$) | 3275 ± 253 | 753 ± 45 | 1048 ± 68 | < 0.01 | Down-regulated | 46.915 | 6.53 | Intermediary metabolism |
| 94 | β-Tropomyosin (TPM2) | 2356 ± 32 | 754 ± 75 | 518 ± 32 | < 0.05 | Down-regulated | 29.980 | 4.66 | Structural protein |
| 100 | WD repeat domain 1 (WDR1) | 1456 ± 124 | 495 ± 34 | 408 ± 35 | < 0.01 | Down-regulated | 66.836 | 6.17 | Structural protein |

hMSCs, human mesenchymal stem cells; hTERT, human telomerase reverse transcriptase.

 *Cell Proliferation*, **41**, 625–644.

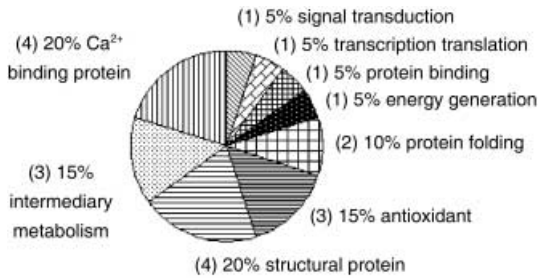


**Figure 4. Pie chart representing distribution of the 20 differentially expressed proteins in hTERT–hMSCs in comparison to primary hMSCs, according to their biological functions.** Numbers in the brackets represent the number of identified proteins. hMSCs, human mesenchymal stem cells; hTERT, human telomerase reverse transcriptase.

**Verification of differentially expressed proteins by Western blotting analysis and RT-PCR**

To confirm changes of protein expression in hTERT–hMSCs, we performed Western blot and RT-PCR analyses for some of the differentially expressed proteins. In Western blot analyses, the protein levels of annexin A1, annexin A2, annexin V and GSTP1 decreased and those of TUBA1B, RCN1, CCT6A and ACTG1 increased in hTERT–hMSCs at PD 95 and PD 275 in comparison with primary hMSCs at PD 12 ($P < 0.05$), but there was no significant difference of these protein levels between hTERT–hMSCs at PD 95 and PD 275 ($P > 0.05$). We detected no change in protein level of prohibitin and p53 between hTERT–hMSCs and primary hMSCs ($P > 0.05$). These results were identical to those of the proteome analysis and indicated that proteomic analysis of primary hMSCs and hTERT–hMSCs was legitimate. In the RT-PCR analyses, RNA level of annexin A2 decreased and those of TUBA1B, CCT6A increased in the hTERT–hMSCs in comparison with primary hMSCs ($P < 0.05$). In addition, no change of RNA levels of prohibitin or p53 between hTERT–hMSCs and primary hMSCs were detected ($P > 0.05$). These results were identical to those of the Western blot analysis. However, we could detect no variations in mRNA levels of annexin A1, annexin V, RCN1 and GSTP1. The change of annexin A1, annexin V, RCN1 and GSTP1 protein levels between primary hMSCs and hTERT–hMSCs did not correlate with those of mRNA levels (Fig. 5), indicating that changes of annexin A1, annexin V, RCN1 and GSTP1 between primary hMSCs and hTERT–hMSCs occur at translation or post-translation levels. In other words, introduction of the hTERT gene into hMSCs did not result in changes of annexin A1, annexin V, GSTP1 and RCN1 mRNA expression although there was a decrease in protein levels of annexin A1, annexin V and GSTP1, while there was an increase in protein level of RCN1 that must have occurred during translation or post-translation.

## DISCUSSION

In the present study, we rebuilt telomerase activity of hMSCs and prolonged their lifespan through ectopic expression of hTERT, by using recombinant retroviruses with the *hTERT* gene. After cloning using the limited dilution method, hTERT–hMSCs were continuously passaged over 290 PDs (Huang *et al*. 2007). Here, we have performed proteomic analysis of hTERT–hMSCs at PD 95 and PD 275 and primary hMSCs at PD 12 to characterize the established cell line. Protein profiles of primary hMSCs and hTERT–hMSCs were compared and 20 differentially

 

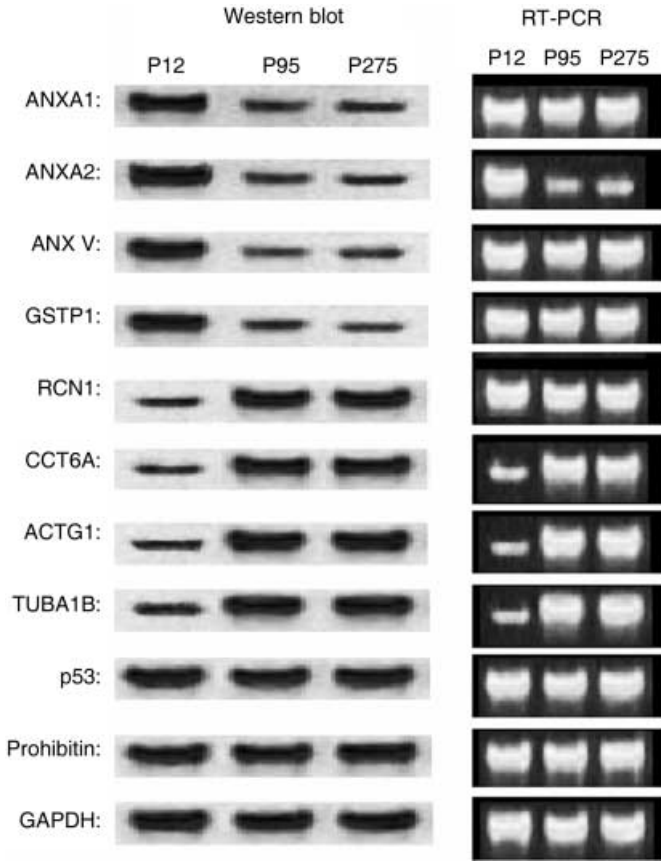


**Figure 5. Confirmation of differentially expressed proteins in hTERT–hMSCs at PD 95 and PD 275 in comparison with primary hMSCs at PD 12, using RT-PCR and Western blot analysis.** Semiquantitative RT-PCR analysis of genes shown to confirm differentially regulated protein/genes in hTERT–hMSCs. Equal aliquots of total RNA were reverse transcribed and amplified with primers specific for annexin A1, annexin A2, annexin V, GSTP1, RCN1, CCT6A, ACTG1, TUBA1B, p53 and prohibitin using GAPDH as a control. Western blot analysis showed differential regulation of annexin A1, annexin A2, annexin V, GSTP1, RTN1, CCT6A, ACTG1, TUBA1B, p53 and prohibitin using GAPDH as control. hMSCs, human mesenchymal stem cells; hTERT, human telomerase reverse transcriptase.

expressed proteins were identified from 2-DE and were grouped into nine categories according to their functions, as documented in Swiss-Prot, NCBI. However, there were no significant differences of these 20 protein expressions during proliferation of hTERT–hMSCs. The proteins were involved in cell functions of protein folding, protein binding, structural protein, energy generation, transcription translation, antioxidant functions, signal transduction, intermediary metabolism and $Ca^{2+}$ binding.

Annexin A1, a calcium-dependent protein, is involved in regulation of cell growth, differentiation and apoptosis. It is one of the phospholipid-binding protein family that has diverse cell functions, including phospholipase A2 inhibition, adhesion and interaction with cytoskeletal proteins (Raynal & Pollard 1994). It plays an important role in cell processes of hMSCs through the $Ca^{2+}$ signalling pathway (Kawano *et al*. 2002). It has been reported that annexin A1 had a cell-type

independent, antiproliferation function through sustaining activation of the extracellular signal-regulated kinase (ERK) signalling cascade. Annexin A1 reduces cell proliferation by ERK-mediated disruption of the actin cytoskeleton and ablation of cyclin $D_1$ protein expression. In the present study, annexin A1 was detected in primary MSCs, but its expression in hTERT–hMSCs showed down-regulation. Expression of actin cytoskeleton in hTERT–hMSCs increased in accompaniment with down-regulation of annexin A1. These results suggest that hTERT–hMSCs sustain the capacity of proliferation through decrease of annexin A1 level.

Reticulocalbin 1 is also a calcium-binding protein; it is located in the endoplasmic reticulum (Ozawa & Muramatsu 1993). Deletion of RCN1 causes early death of small eye Harwell mouse homozygotes, suggesting that RCN1 is essential for cell life (Kent *et al*. 1997). Liu *et al*. (1997) have reported that RCN1 transcripts were overexpressed in a highly invasive breast cancer cell line but not in a poorly invasive one. In hydrogen peroxide-resistant cells, the transmembrane potential of endoplasmic reticulum proteins requires additional storage of millimolar amounts of calcium in the endoplasmic reticulum in contrast to micromolar amounts in the cytosol (Carper *et al*. 2001). Increase of RCN1 transcripts reflects a change in $Ca^{2+}$ gradient. We detected up-regulation of RCN1 in hTERT–hMSCs in comparison with primary hMSCs, although levels of RCN1 between hTERT–hMSCs at PD 95 and PD 275 showed little variation. Therefore, RCN1 should be essential for proliferation of hTERT–hMSCs.

In the present study, a significant down-regulation of GSTP1 was detected in hTERT–hMSCs in comparison with primary hMSCs. There was no significant change of GSTP1 between hTERT–hMSCs at PD 95 and PD275. Telomere integrity and nuclear export of hTERT are affected by chronic oxidative stress that forces cells to enter into replicative senescence (Haendeler *et al*. 2004; Kurz *et al*. 2004). GSTP1 can be used as a marker to predict enhanced oxidative stress in cells (Nagai *et al*. 2004). GSTP1 was also found to have higher expression in pituitaries of old mice in comparison to young mice (Marzban *et al*. 2002). The down-regulation of GSTP1 expression implies less oxidative stress in hTERT–hMSCs than that in the primary hMSCs. Thus, it suggests that hTERT–hMSCs suffer less oxidative stress in order to sustain high telomerase activity.

Expression of chaperonin-containing T-complex polypeptide 1 (CCT) was strongly up-regulated during cell proliferation, especially from $G_1$/S to early S phase. CCT plays an important role in cell growth as it assists folding of actin, tubulin and other proteins to attain their functional conformations (Ellis & van der Vies 1991; Frydman *et al*. 1992; Gao *et al*. 1992; Gething & Sambrook 1992; Sternlicht *et al*. 1993; Tian *et al*. 1995; Hartl 1996; Vainberg *et al*. 1998; Siegers *et al*. 1999; Thulasiraman *et al*. 1999). CCT expression is down-regulated in $G_0$/$G_1$ phase of the cell cycle. It can be down-regulated by agents affecting cell growth and differentiation such as interferon γ and okadaic acid (Hynes *et al*. 1996). When tubulin is rapidly synthesized and assembled, CCT expression is up-regulated (Willison *et al*. 1990; Soares *et al*. 1994; Roobol *et al*. 1995; Cyrne *et al*. 1996). Apart from such cases, the primary cause for promoting CCT expression seems to be continuous cell growth. Yokota supposed that CCT should assist maturation of proteins up-regulated at $G_1$/S transition and/or early S phase (Yokota *et al*. 1999). Here, expression of TUBA1B and ACTG1 was significantly up-regulated in hTERT–hMSCs in comparison with primary hMSCs. Significant up-regulation of CCT6A expression in the hTERT–hMSCs also was detected. It can be supposed that transduction of hTERT into hMSCs irritates CCT expression which assists folding of actin, tubulin and other proteins to attain functional conformations and to increase growth rate of hTERT–hMSCs.

The protein prohibitin plays an important role in control of the $G_1$/S phase and interacts with the retinoblastoma protein. It is associated with mitochondria and has the ability to inhibit apoptosis (Fusaro *et al*. 2002). Senescent cells have been shown to down-regulate prohibitin

 

expression (Coates *et al*. 2001). Prohibitin can also be found in the nucleus where it can bind to the tumour suppressor p53 and induce p53 transcription (Fusaro *et al*. 2003). The p53 is a tumour suppressor affecting cell growth and it plays a pivotal role in cellular responses to genotoxic damage and other forms of stress (Levine 1997; Vogelstein *et al*. 2000). When DNA is damaged, p53 induces growth arrest to facilitate DNA repair (MacLachlan *et al*. 2002; Fei & El-Deiry 2003). In the present study, significantly up-regulated or down-regulated prohibitin expression in hTERT–hMSCs in comparison to primary hMSCs was not detected. Otherwise, p53 protein expression in the three kinds of cells showed no variation in the Western blot analysis. Thus, it can be suggested that sustaining a consistent level of prohibitin causes a concomitant sustained level of p53 expression and that prohibitin and p53 keep hTERT–hMSCs in a non-transforming status.

In conclusion, this study has described a proteomics approach to understanding the molecular mechanism of immortalization of hMSCs transduced with hTERT. Protein identification demonstrates that hTERT affects many aspects of cellular functions. Using this method, we identified 20 proteins relative to proliferation and transformation of cells. These protein expressions were altered in hTERT–hMSCs in comparison to primary hMSCs, but stabilized during proliferation of hTERT–hMSCs, which may result in immortalization and non-transformation of hMSCs. It was a regrettable fact that we could not compare the proteomic profiles of primary hMSCs and hTERT–hMSCs at an equal passage. Primary hMSCs lose their differentiation potential after PD 15 and undergo senescence-associated proliferation arrest after PD25. Thus, it is impossible to obtain primary hMSCs at higher passages for proteomic analysis. Moreover, hTERT–hMSCs from cell clones need to be proliferated through many passages to obtain enough cells for proteomic analysis. Due to these limitations, it was difficult to compare the proteomic profiles of primary hMSCs and hTERT–hMSCs at the same passage. As a remedy to difference in analysis, we analyse the proteomic profile of hTERT–hMSCs at PD 275 for an additional issue of proteomic dynamics during cell proliferation. Our data provide a preliminary outline for further studies of the detailed mechanism. Further investigation is required to determine the roles of the identified proteins in cell proliferation or tumorigenesis through some approaches, such as the knockdown technique (e.g. using retroviral shRNAi) of key identified genes proposed to be important in hTERT-induced immortalization of the hMSCs.

## ACKNOWLEDGEMENTS

We would like to thank Mr. Chris Wood of Zhejiang University for critical reading of the manuscript. This work was supported in part by grants from the National Nature foundation of China (30671071) and Zhejiang Scientific Foundation (no. 2003C23015).

## REFERENCES

Bernardo ME, Avanzini MA, Perotti C, Cometa AM, Moretta A, Lenta E, Del Fante C, Novara F, de Silvestri A, Amendola G (2006) Optimization of *in vitro* expansion of human multipotent mesenchymal stromal cells for cell-therapy approaches: further insights in the search for a fetal calf serum substitute. *J. Cell. Physiol*. **211**, 121–130.

Burns JS, Abdallah BM, Guldberg P, Rygaard J, Schroder HD, Kassem M (2005) Tumorigenic heterogeneity in cancer stem cells evolved from long-term cultures of telomerase-immortalized human mesenchymal stem cells. *Cancer Res*. **65**, 3126–3135.

Campisi J (1997) The biology of replicative senescence. *Eur. J. Cancer* **33**, 703–709.

 

Caplan AI (1991) Mesenchymal stem cells. *J. Orthop. Res*. **9**, 641–650.
Caplan AI, Bruder SP (2001) Mesenchymal stem cells: building blocks for molecular medicine in the 21st century. *Trends Mol. Med*. **7**, 259–264.
Carper D, John M, Chen Z, Subramanian S, Wang R, Ma W, Spector A (2001) Gene expression analysis of an $H_2O_2$-resistant lens epithelial cell line. *Free Radic. Biol. Med*. **31**, 90–97.
Coates PJ, Nenutil R, McGregor A, Picksley SM, Crouch DH, Hall PA, Wright EG (2001) Mammalian prohibitin proteins respond to mitochondrial stress and decrease during cellular senescence. *Exp. Cell Res*. **265**, 262–273.
Cyrne L, Guerreiro P, Cardoso AC, Rodrigues-Pousada C, Soares H (1996) The Tetrahymena chaperonin subunit CCT eta gene is coexpressed with CCT gamma gene during cilia biogenesis and cell sexual reproduction. *FEBS Lett*. **383**, 277–283.
Deans RJ, Moseley AB (2000) Mesenchymal stem cells: biology and potential clinical uses. *Exp. Hematol*. **28**, 875–884.
Dennis JE, Caplan AI (1996) Differentiation potential of conditionally immortalized mesenchymal progenitor cells from adult marrow of an H-2KbtsA58 transgenic mouse. *J. Cell. Physiol*. **167**, 523–538.
Ellis RJ, van der Vies SM (1991) Molecular chaperones. *Annu. Rev. Biochem*. **60**, 321–347.
Fei P, El-Deiry WS (2003) P53 and radiation responses. *Oncogene* **22**, 5774–5783.
Feldmann RE, Bieback K, Maurer MH, Kalenka A, Bürgers HF, Gross B, Hunzinger C, Klüter H, Kuschinsky W, Eichler H (2005) Stem cell proteomes: a profile of human mesenchymal stem cells derived from umbilical cord blood. *Electrophoresis* **26**, 2749–2758.
Frydman J, Nimmesgern E, Erdjument-Bromage H, Wall JS, Tempst P, Hartl FU (1992) Function in protein folding of TRiC, a cytosolic ring complex containing TCP-1 and structurally related subunits. *EMBO J*. **11**, 4767–4778.
Fusaro G, Dasgupta P, Rastogi S, Joshi B, Chellappan S (2003) Differential regulation of Rb family proteins and prohibitin during camptothecin-induced apoptosis. *J. Biol. Chem*. **278**, 47853–47861.
Fusaro G, Wang S, Chellappan S (2002) Differential regulation of Rb family proteins and prohibitin during camptothecin-induced apoptosis. *Oncogene* **21**, 4539–4458.
Gao Y, Thomas JO, Chow RL, Lee GH, Cowan NJ (1992) A cytoplasmic chaperonin that catalyzes beta-actin folding. *Cell* **69**, 1043–1050.
Gething MJ, Sambrook J (1992) Protein folding in the cell. *Nature* **355**, 33–45.
Gharahdaghi F, Weinberg CR, Meagher DA, Imai BS, Mische SM (1999) Mass spectrometric identification of proteins from silver-stained polyacrylamide gel: a method for the removal of silver ions to enhance sensitivity. *Electrophoresis* **20**, 601–605.
Gimeno MJ, Maneiro E, Rendal E, Ramallal M, Sanjurjo L, Blanco FJ (2005) Cell therapy: a therapeutic alternative to treat focal cartilage lesions. *Transplant. Proc*. **37**, 4080–4083.
Gorg A, Obermaier C, Boguth G, Harder A, Scheibe B, Wildgruber R, Weiss W (2000) The current state of two dimensional electrophoresis with immobilized pH gradients. *Electrophoresis* **21**, 1037–1053.
Haendeler J, Hoffmann J, Diehl JF, Vasa M, Spyridopoulos I, Zeiher AM, Dimmeler S (2004) Antioxidants inhibit nuclear export of telomerase reverse transcriptase and delay replicative senescence of endothelial cells. *Circ. Res*. **94**, 768–775.
Hartl FU (1996) Molecular chaperones in cellular protein folding. *Nature* **381**, 571–579.
Hayflick L (1976) The cell biology of human aging. *N. Engl. J. Med*. **295**, 1302–1308.
Huang GP, Zheng Q, Sun J, Guo CJ, Yang JF, Chen R, Xu YL, Wang GZ, Shen D, Pan ZJ, Jin J, Wang JF (2008) Stabilization of cellular properties and differentiation mutilpotential of human mesenchymal stem cells transduced with hTERT gene in a long-term culture. *J. Cell. Biochem*. **103**, 1256–1269.
Hynes G, Celis JE, Lewis VA, Carne A, U S, Lauridsen JB, Willison KR (1996) Analysis of chaperonin-containing TCP-1 subunits in the human keratinocyte two-dimensional protein database: further characterisation of antibodies to individual subunits. *Electrophoresis* **17**, 1720–1727.
Jaiswal N, Haynesworth SE, Caplan AI, Bruder SP (1997) Osteogenic differentiation of purified, culture-expanded human mesenchymal stem cells *in vitro*. *J. Cell. Biochem*. **64**, 295–312.
Javazon EH, Colter DC, Schwarz EJ, Prockop DJ (2001) Rat marrow stromal cells are more sensitive to plating density and expand more rapidly from single-cell-derived colonies than human marrow stromal cells. *Stem Cells* **19**, 219–225.
Jiang Y, Jahagirdar BN, Reinhardt RL, Schwartz RE, Keene CD, Ortiz-Gonzalez XR, Reyes M, Lenvik T, Lund T, Du Blackstad MJ, Aldrich S, Lisberg A, Low WC, Largaespada DA, Verfaillie CM, Verfaillie CM (2002) Pluripotency of mesenchymal stem cells derived from adult marrow. *Nature* **418**, 41–49.
Kawano S, Shoji S, Ichinose S, Yamagata K, Tagami M, Hiraoka M (2002) Characterization of $Ca^{2+}$ signaling pathways in human mesenchymal stem cells. *Cell Calcium* **32**, 165–174.
Kent J, Lee M, Schedl A, Boyle S, Fante J, Powell M, Rushmere N, Abbott C, van Heyningen V, Bickmore WA (1997) The reticulocalbin gene maps to the WAGR region in human and to the small eye Harwell deletion in mouse. *Genomics* **42**, 260–267.

 

Kurz DJ, Decary S, Hong Y, Trivier E, Akhmedov A, Erusalimsky JD (2004) Chronic oxidative stress compromises telomere integrity and accelerates the onset of senescence in human endothelial cells. *J. Cell Sci*. **117**, 2417–2426.

Levine AJ (1997) p53, the cellular gatekeeper for growth and division. *Cell* **88**, 323–331.

Liu Z, Brattain MG, Appert H (1997) Differential display of reticulocalbin in the highly invasive cell, MDA-MB-435, versus the poorly invasive cell line, MCF-7. *Biochem. Biophys. Res. Commun*. **231**, 283–289.

Mackay AM, Beck SC, Murphy JM, Barry FP, Chichester CO, Pittenger MF (1998) Chondrogenic differentiation of cultured human mesenchymal stem cells from marrow. *Tissue Eng*. **4**, 415–428.

MacLachlan TK, Takimoto R, El-Deiry WS (2002) BRCA1 directs a selective p53-dependent transcriptional response towards growth arrest and DNA repair targets. *Mol. Cell. Biol*. **22**, 4280–4292.

Marzban G, Grillari J, Reisinger E, Hemetsberger T, Grabherr R, Katinger H (2002) Age-related alterations in the protein expression profile of C57BL/6J mouse pituitaries. *Exp. Gerontol*. **37**, 1451–1460.

Maurer MH, Feldmann RE Jr, Futterer CD, Butlin J, Kuschinsky W (2004) Comprehensive proteome expression profiling of undifferentiated versus differentiated neural stem cells from adult rat hippocampus. *Neurochem. Res*. **29**, 1129–1144.

Nagai F, Kato E, Tamura HO (2004) Oxidative stress induces GSTP1 and CYP3A4 expression in the human erythroleukemia cell line, K562. *Biol. Pharm. Bull*. **27**, 492–495.

Ozawa M, Muramatsu T (1993) Reticulocalbin, a novel endoplasmic reticulum resident Ca21-binding protein with multiple EF-hand motifs and a carboxyl-terminal HDEL sequence. *J. Biol. Chem*. **268**, 699–705.

Perkins DN, Pappin DJ, Creasy DM, Cottrell JS (1999) Probability-based protein identification by searching sequence databases using mass spectrometry data. *Electrophoresis* **20**, 3551–3567.

Pittenger MF, Mackay AM, Beck SC, Jaiswal RK, Douglas R, Mosca JD, Moorman MA, Simonetti DW, Craig S, Marshak DR (1999) Multilineage potential of adult human mesenchymal stem cells. *Science* **284**, 143–147.

Prockop DJ (1997) Marrow stromal cells as stem cells for nonhematopoietic tissues. *Science* **276**, 71–74.

Qiu LY, Wang JF, Shen D, Jin J (2004) Expansion and chondrogenic induction of human bone marrow mesenchymal stem cells. *J. Zhejiang Univer. Sci*. **31**, 337–342.

Ramagli LS (1999) Quantifying protein in 2-D PAGE solubilization buffers. *Methods Mol. Biol*. **112**, 99–103.

Raynal P, Pollard HB (1994) Annexins: the problem of assessing the biological role for a gene family of multifunctional calcium- and phospholipid-binding proteins. *Biochim. Biophys. Acta* **1197**, 63–93.

Roobol A, Holmes FE, Hayes NV, Baines AJ, Carden MJ (1995) Cytoplasmic chaperonin complexes enter neurites developing *in vitro* and differ in subunit composition within single cells. *J. Cell Sci*. **108**, 1477–1488.

Shevchenko A, Wilm M, Vorm O, Mann M (1996) Mass spectrometric sequencing of proteins silver-stained polyacrylamide gels. *Anal. Chem*. **68**, 850–858.

Shi S, Gronthos S, Chen S, Reddi A, Counter CM, Robey PG, Wang CY (2002) Bone formation by human postnatal bone marrow stromal stem cells is enhanced by telomerase expression. *Nat. Biotechnol*. **20**, 587–591.

Siegers K, Waldmann T, Leroux MR, Grein K, Shevchenko A, Schiebel E, Hartl FU (1999) Compartmentation of protein folding in vivo: sequestration of non-native polypeptide by the chaperonin-GimC system. *EMBO J*. **18**, 75–84.

Simonsen JL, Rosada C, Serakinci N, Justesen J, Stenderup K, Rattan SI, Jensen TG, Kassem M (2002) Telomerase expression extends the proliferative life-span and maintains the osteogenic potential of human bone marrow stromal cells. *Nat. Biotechnol*. **20**, 592–596.

Soares H, Penque D, Mouta C, Rodrigues-Pousada C (1994) A Tetrahymena orthologue of the mouse chaperonin subunit CCT gamma and its coexpression with tubulin during cilia recovery. *J. Biol. Chem*. **269**, 29299–29307.

Stenderup K, Justesen J, Clausen C, Kassem M (2003) Aging is associated with decreased maximal life span and accelerated senescence of bone marrow stromal cells. *Bone* **33**, 919–926.

Sternlicht H, Farr GW, Sternlicht ML, Driscoll JK, Willison K, Yaffe MB (1993) The t-complex polypeptide 1 complex is a chaperonin for tubulin and actin *in vivo*. *Proc. Natl. Acad. Sci. USA* **90**, 9422–9426.

Thulasiraman V, Yang CF, Frydman J (1999) *In vivo* newly translated polypeptides are sequestered in a protected folding environment. *EMBO J*. **18**, 85–95.

Tian G, Vainberg IE, Tap WD, Lewis SA, Cowan NJ (1995) Specificity in chaperonin-mediated protein folding. *Nature* **375**, 250–253.

Vainberg IE, Lewis SA, Rommelaere H, Ampe C, Vandekerckhove J, Klein HL, Cowan NJ (1998) Prefoldin, a chaperone that delivers unfolded proteins to cytosolic chaperonin. *Cell* **93**, 863–873.

Vogelstein B, Lane D, Levine AJ (2000) Surfing the p53 network. *Nature* **408**, 307–310.

Vogt JA, Schroer K, Holzer K, Hunzinger C, Klemm M, Biefang-Arndt K, Schillo S, Cahill MA, Schrattenholz A, Matthies H, Stegmann W (2003) Protein abundance quantification in embryonic stem cells using incomplete metabolic labelling with 15N amino acids, matrix-assisted laser desorption/ionisation timeofflight mass spectrometry, and analysis of relative isotopologue abundances of peptides. *Rapid Commun. Mass Spectrom*. **17**, 1273–1282.

Wakitani S, Saito T, Caplan AI (1995) Myogenic cells derived from rat bone marrow mesenchymal stem cells exposed to 5-azacytidine. *Muscle Nerve* **18**, 1417–1426.

Willison KR, Hynes G, Davies P, Goldsborough A, Lewis VA (1990) Expression of three t-complex genes, Tcp-1, D17Leh117c3, and D17Leh66, in purified murine spermatogenic cell populations. *Genet. Res*. **56**, 193–201.

Xiang Y, Zheng Q, Jia BB, Huang GP, Xie CG, Pan ZJ, Wang JF (2007) *Ex vivo* expansion, adipogenesis and neurogenesis of cryopreserved human bone marrow mesenchymal stem cells. *Cell Biol. Int*. **31**, 444–450.

Yokota S, Yanagi H, Yura T, Kubota H (1999) Cytosolic chaperonin is up-regulated during cell growth. Preferential expression and binding to tubulin at G(1)/S transition through early S phase. *J. Biol. Chem*. **274**, 37070–37078.

Zhu LH, Zhou TJ, Shi GY, Zhang GL, Li SY (2007) Expression of bcl-2 gene in EBV-transformed human gastric epithelial cell line GES-1. *Nan Fang Yi Ke Da Xue Xue Bao* **27**, 195–197.

 